AGU100 ADVANCING EARTH AND SPACE SCIENCE

Water Resources Research

RESEARCH ARTICLE
10.1029/2018WR024098

Restoring a Natural Fire Regime Alters the Water Balance of a Sierra Nevada Catchment

Gabrielle F. S. Boisramé[1,2], Sally E. Thompson[3], Christina (Naomi) Tague[4], and Scott L. Stephens[1]

[1]Department of Environmental Science, Policy, and Management, University of California, Berkeley, CA, USA, [2]Division of Hydrologic Sciences, Desert Research Institute, Las Vegas, NV, USA, [3]Department of Civil and Environmental Engineering, University of California, Berkeley, CA, USA, [4]Bren School of Environmental Science and Management, University of California, Santa Barbara, CA, USA

Key Points:
- Fire suppression has altered vegetation cover in Sierra Nevada watersheds, affecting water balance
- Models show that mixed-severity fires lead to increased snowpack, annual streamflow, and water storage
- Most changes in the water balance due to fire were more pronounced in wet years compared to dry years

Supporting Information:
- Supporting Information S1

Correspondence to:
G. F. S. Boisramé,
gboisrame@berkeley.edu

Citation:
Boisramé, G. F. S., Thompson, S. E., Tague, C., & Stephens, S. L. (2019), Restoring a natural fire regime alters the water balance of a Sierra Nevada catchment. *Water Resources Research*, *55*, 5751–5769. https://doi.org/10.1029/2018WR024098

Received 14 SEP 2018
Accepted 7 JUN 2019
Accepted article online 26 JUN 2019
Published online 18 JUL 2019

Abstract Fire suppression in western U.S. mountains has caused dense forests with high water demands to grow. Restoring natural wildfire regimes to these forests could affect hydrology by changing vegetation composition and structure, but the specific effects on water balance are unknown. Mountain watersheds supply water to much of the western United States, so understanding the relationship between fire regime and water yield is essential to inform management. We used a distributed hydrological model to quantify hydrologic response to a restored fire regime in the Illilouette Creek Basin (ICB) within Yosemite National Park, California. Over the past 45 years, as successive fires reduced the ICB's forest cover approximately 25%, model results show that annual streamflow, subsurface water storage, and peak snowpack increased relative to a fire-suppressed control, while evapotranspiration and climatic water deficit decreased. A second model experiment compared the water balance in the ICB under two vegetation cover scenarios: 2012 vegetation, representing a frequent-fire landscape, and 1969 vegetation, representing fire suppression. These two model landscapes were run with observed weather data from 1972 to 2017 in order to capture natural variations in precipitation and temperature. This experiment showed that wet years experienced greater fire-related reductions in evapotranspiration and increases in streamflow, while reductions in climatic water deficit were greater in dry years. Spring snowmelt runoff was higher under burned conditions, while summer baseflow was relatively unaffected. Restoring wildfire to the fire-suppressed ICB likely increased downstream water availability, shifted streamflows slightly earlier, and reduced water stress to forests.

1. Introduction

Mountain watersheds are vital sources of water, the availability of which is sensitive to changes in climate and vegetation cover (Bladon et al., 2014; Tague & Dugger, 2010). Since the early twentieth century, a policy of fire suppression in the mountains of the western United States has increased forest density in many areas relative to its natural condition, especially in forests adapted to frequent fire (Collins et al., 2011; Miller et al., 2012). Denser forests are believed to contribute to water scarcity and fire risk, stresses which are expected to worsen in a warming climate (Boisramé et al., 2017; Department of Water Resources, 2008; Dettinger et al., 2004; Westerling & Bryant, 2008). Although reintroducing wildfire to such landscapes might be expected to alleviate water stress (and reduce fire hazards; Collins et al., 2009), in practice little is known about the long-term effects of restoring a frequent, mixed-severity fire regime on forest water balance. In part, this knowledge gap reflects a dearth of experimentation with restoring natural wildfire. An exception is in the Illilouette Creek Basin (ICB) in Yosemite National Park. ICB was fire-suppressed for nearly a hundred years during which only 8 ha burned (Collins & Stephens, 2007). Since 1972, however, the basin has been subject to "Natural Fire Management" policy (van Wagtendonk, 2007). In the ICB, lightning-ignited fires are allowed to burn unless specific risks require intervention (van Wagtendonk, 2007). The fires have reduced forest cover by ≈25% (Boisramé et al., 2017; Boisramé et al., 2017). Shrubland, sparse meadows, and wet meadows have replaced the tree cover (Figure 1 ; Boisramé, Thompson, Kelly, et al., 2017). The altered fire regime has also changed forest stand structure by increasing the heterogeneity in tree size, basal area, and canopy cover (Collins & Stephens, 2010; Collins et al., 2016).

Plants regulate soil structure, transpiration, interception, and shade (Brown et al., 2005), meaning that changes in vegetation cover and structure can induce multiple related, and potentially confounding, shifts in

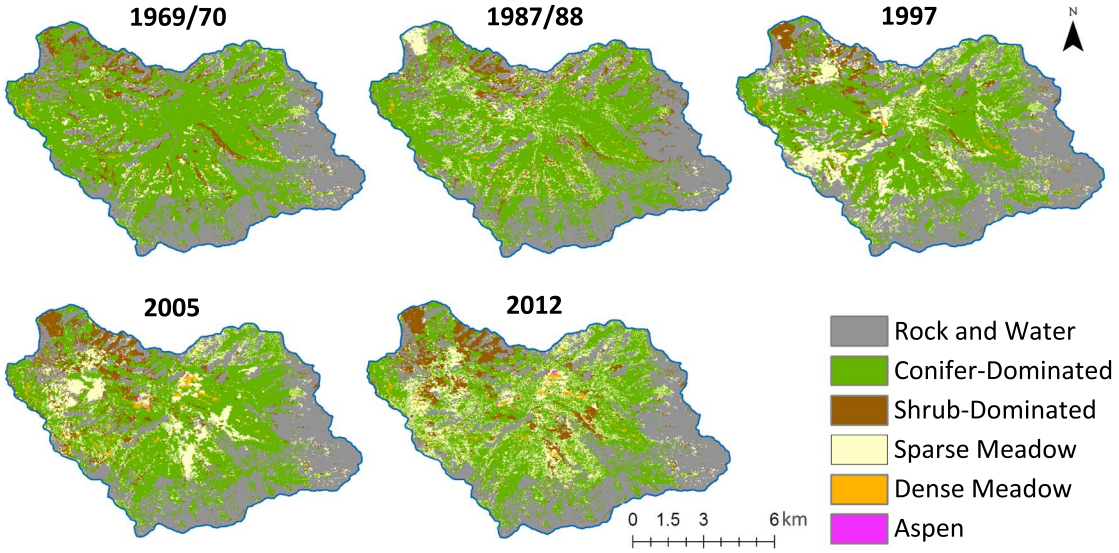

Figure 1. Vegetation maps of the Illilouette Creek Basin spanning the range from 1969 (fire-suppressed conditions) to 2012 (after 40 years of wildfires). Figure details are in Boisramé, Thompson, Kelly, et al. (2017).

water balance (Bart et al., 2016; Lundquist et al., 2013). In snow-dominated systems, for example, an intact forest canopy intercepts falling snow and shortwave radiation while providing a source of longwave radiation to the snowpack. Interception reduces snowpack accumulation, while both shortwave and longwave radiation cause snowmelt and sublimation. Multiple studies have found reductions in modeled sublimation from the canopy following leaf area index (LAI) reductions, while modeled sublimation from the snowpack on the ground either increased or decreased depending on weather, topography, and original canopy density (e.g., Frank et al., 2019; Svoma, 2017). Thus, removal of a canopy can result in either increases or decreases in snowpack, depending on exactly which snow loss processes are most altered. The net impact depends on local factors such as temperature, solar radiation, and the geometry of canopy openings (Bart et al., 2016; Lundquist et al., 2013; Micheletty et al., 2014; Stevens, 2017; Tennant et al., 2017). Similar confounding processes affect summer soil moisture, as dense canopies can reduce water stores by intercepting rainfall and transpiring actively, but also shade the soil, reducing soil evaporation. In spite of these confounding factors, previous work in the Sierra Nevada suggests that individual fires can induce net increases in streamflow (Bales et al., 2018; Saksa, 2015).

Patterns of repeat wildfire, however, do not only change vegetation at a point but across entire landscapes and with considerable spatiotemporal variation. Fire increases landscape heterogeneity (Boisramé et al., 2017; Stephens et al., 2008), which can, for example, lengthen the snowmelt period relative to homogeneous land cover (Ellis et al., 2013; Kattelmann et al., 1983). However, if fire occurrence is biased in space—for instance, to preexisting dry, water-limited regions—the scope for water balance change at basin scale is reduced (Roche et al., 2018; Saksa et al., 2017). Large-scale fire-induced vegetation change is well known to increase runoff generation (Brown et al., 2005; Helvey, 1980; Mayor et al., 2007; Pierson et al., 2001), but regrowth and forest succession mean that this effect is transient (Lane et al., 2010; Neary et al., 2005; Wine & Cadol, 2016). Since the magnitude of hydrological response to fire is also dependent on weather (Roche et al., 2018), there is considerable uncertainty about the intensity and persistence of these transient effects. Thus, while restoring the ICB's frequent fire regime has reduced forest cover and density, which would be expected to make the basin wetter, predicting the long-term water balance response remains challenging.

Ideally, water balance responses to changing fire regimes would be empirically quantified, but in practice the data available to support such empirical analyses are limited. The nearest stream gauging point to the ICB is located after the confluence of Illilouette Creek with the Upper Merced River (UMR; Figure 2a; Boisramé, Thompson, Collins, & Stephens, 2017). Previous empirical work suggested a slight increase (at least 3%) in UMR annual streamflow due to the restored fire regime in the ICB (Boisramé, Thompson, Collins, & Stephens, 2017). This estimate, however, is confounded by interannual weather variations and the difficulty of extracting the signal of change in the ICB from the total UMR flow. This study therefore uses mechanistic

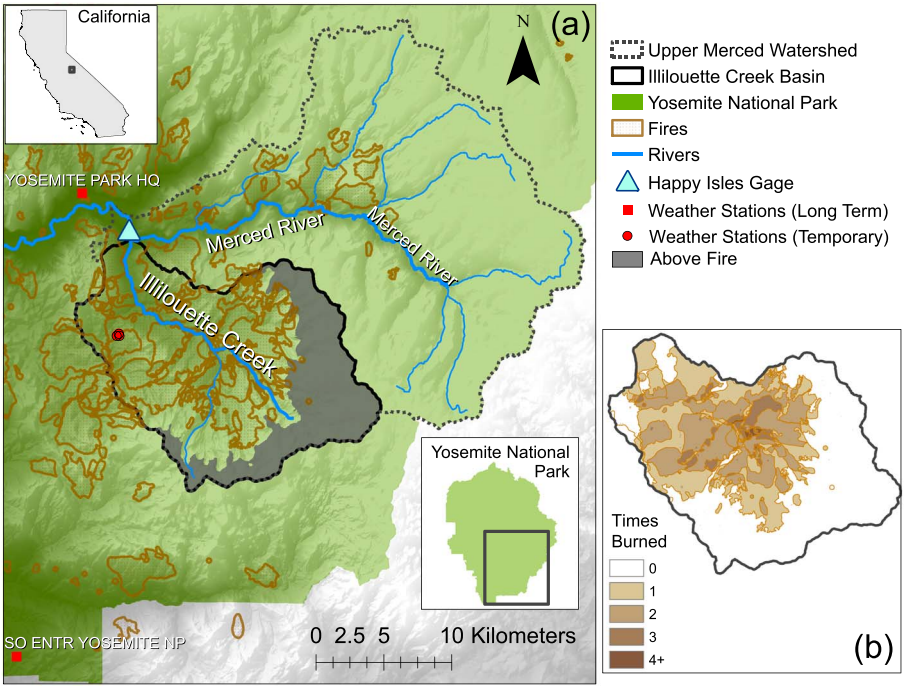

Figure 2. (a) Location of the Upper Merced Watershed, Illilouette Creek Basin, Happy Isles stream gage, and weather stations. The main stems of the Merced River and Illilouette Creek, along with their major tributaries, are also shown. All fires from 1974 to 2012 are shown with outlines and texture within the fire boundary. The grayed-out region within ICB indicates the area above elevations influenced by wildfire; this area was omitted when calculating changes per unit area. (b) Map of the number of times each part of the ICB has burned since 1972. For a more detailed fire map, see Figure S7.

modeling, specifically the Regional Hydro-Ecologic Simulation System (RHESSys) model, to better understand fire-induced hydrologic change in the ICB. RHESSys provides a spatially distributed representation of snow, water, energy, and vegetation dynamics (Tague & Band, 2004) at the level of detail needed to describe mountain ecohydrology (Lundquist & Loheide, 2011). RHESSys has been extensively used in previous studies of hydrologic changes in the Sierra Nevada (Christensen et al., 2008; Tague & Peng, 2013), including changes related to fire (Saksa, 2015).

Previous modeling efforts linking fire and water focused primarily on individual fires and their aftermath (e.g., Seibert et al., 2010; Vieira et al., 2015), and the few studies that considered repeated fire occurrence relied on synthetic fire regimes (e.g., Miller & Urban, 2000; Ursino & Rulli, 2011). In contrast, our study combines historical vegetation and climate data with hydrologic modeling to explore the impacts of a real fire *regime* over multiple decades. Our study consists of two experiments that aim to first quantify the history of water balance change experienced in the ICB since the institution of the managed wildfire policy and second to explore the range of possible water balance changes that could arise in the ICB between fire-suppressed and fire-impacted conditions, subject to observed interannual climate variability. This second experiment provides a benchmark for the order of magnitude, variability, and climate dependence of water balance change following 40 years of a restored fire regime.

2. Methods

2.1. Study Area

The ICB is a 150-km^2 basin within the 470-km^2 Upper Merced Watershed (UMW) in Yosemite National Park, California, USA (Figure 2a). The ICB lies in a 1,800- to 3,000-m elevation range, compared to the 1,230- to 3,800-m range of the UMW. The region experiences a Mediterranean climate with cold snowy winters and warm summers. The Yosemite Headquarters weather station in Yosemite Valley (the most complete nearby weather record) shows a mean January daily minimum temperature of −2 °C and mean July daily maximum temperature of 32 °C, with mean annual precipitation of 83 cm/year for water years 1972–2017 (www.ncdc.noaa.gov). According to recent data from temporary weather stations, ICB summer tempera-

tures are approximately 7 °C cooler than in Yosemite Valley, but precipitation and winter temperatures are similar (supporting information Text S1). The basin is covered by coniferous forests (≈ 41% of the watershed, dominated by *Pinus jeffreyi, Abies magnifica, Abies concolor*, and *Pinus contorta*), rocks (≈ 34%), meadows (≈ 16%), and shrublands (≈ 9%, dominated by *Ceanothus cordulatus*; Collins et al., 2007; Boisramé et al., 2017). Under the managed wildfire policy, fire now occurs approximately every 6.8 years in ICB (comparable to an estimated 6.2 years prior to fire suppression; Collins & Stephens, 2007). Fifty-two percent of the total watershed area and ≈75% of the vegetated area has burned at least once since 1972, at a range of fire severities and sizes, leading to a 25% reduction in forest cover between 1972 and 2012 (Figures 2b, S6, and S7; Boisramé, Thompson, Kelly, et al., 2017).

Flow data (1915 to present) are available at the Happy Isles gage (USGS gage 11264500), located downstream of the confluence of Illilouette Creek with the UMR. Mean flow in the UMR at Happy Isles was 11 m^3/s, or 71 cm/year, for 1972–2017 (nwis.waterdata.usgs.gov). These data are supplemented by stream gage data for Illilouette Creek from 2011 onward, which remain uncertain (in terms of absolute magnitudes of flow) due to incomplete calibration of the rating curve for high flows (provided by the Yosemite Resources Management and Science Division).

2.2. RHESSys Model

RHESSys is a spatially distributed model of coupled hydrologic and ecosystem biogeochemical cycling processes. This study used version 5.20.1, run at a daily time step. A detailed description of RHESSys submodels has been provided in previous papers (see C. ; Tague & Band, 2004; C. ; Tague & Peng, 2013). A brief overview of key processes relevant to this study is provided here.

Vertical hydrologic processes in RHESSys include evaporation from canopy, litter and soil layers, sublimation from snow, and transpiration from sunlit and shaded canopy layers, all computed separately using a Penman-Monteith approach (Monteith, 1965). RHESSys implicitly accounts for redistribution of moisture by roots (which has been shown to have important hydrologic impacts in semiarid systems; Prieto et al., 2012) by averaging near-surface soil moisture over plant root depth. For transpiration, soil water content modifies a stomatal conductance term to account for the impact of summer water limitation and accounts for species and soil parameter differences in the water storage-conductance relationship. Shortwave radiation for evapotranspiration (ET) and snow processes is varied spatiotemporally, accounting for slope, aspect, topographic shading, and seasonality. Energy fluxes are attenuated through the canopy as a function of LAI, as are wind speeds. Diffuse and direct radiative fluxes are considered separately. Infiltration of rain throughfall and snowmelt is computed using a Green and Ampt-type approach (Green & Ampt, 1911). Drainage fluxes between subsurface stores (rooting zone, unsaturated, and saturated) are computed as a function of water content and soil parameters. Lateral surface and saturated subsurface water redistribution between spatially explicit patches are based on surface topography and calibrated drainage parameters.

Precipitation and air temperature from point meterologic observations are varied spatially using elevation-specific lapse rates. Incoming precipitation is assumed to be snow for air temperatures below −1 °C and rain for air temperatures above 1 °C and a linear combination between the two temperature thresholds. Canopy interception varies with a species-specific interception capacity per LAI as well as air temperature (following ; Andreadis et al., 2009). Melting and sublimation of intercepted snow varies with air temperature and solar radiation. A fixed daily canopy-snow unloading rate of 1% is also included. Melting and sublimation of snow that reaches the ground is based on a simplified energy budget approach that accounts for shortwave (diffuse and direct) and longwave energy inputs and a temperature-based estimate of latent heat transfers. Capturing all of these processes is important, as sublimation and melt can both cause similar levels of snowpack loss (Bair et al., 2015). Snowpack albedo decays with snowpack age. Of particular relevance for this paper is that higher canopy cover translates to lower shortwave radiation (according to Beer's Law) and increased longwave radiation in the model. Longwave radiation absorbed by the snowpack is estimated as a function of snow and canopy temperatures, canopy cover fraction, snow and canopy emissivities, and downwelling atmospheric longwave radiation. The implementation used here does not vary longwave with LAI or stem density, only with canopy cover. Furthermore, canopy temperatures are assumed to be in equilibrium with surrounding air temperature. The snow model has been evaluated via comparison with point snow measurements (Dugger et al., 2013) and snow on-off imagery for various locations in the western United States. While this snow model provides reasonable estimates of snowmelt rates, it has several limitations. In particular, gap and beneath-canopy wind speeds are not modeled separately within a given patch,

nor does the model account for snow redistribution or variable canopy unloading due to wind. However, we expect that these are secondary to the effects of changing canopy density on the energy budget controls on snow processes.

2.2.1. Model Domain, Parameterization, and Forcing

Lidar elevation data (Kane et al., 2015) were aggregated to 10-m resolution and used to delineate the ICB into hillslopes according to aspect and drainage network and to subdivide hillslopes into patches at 25- or 100-m elevation intervals (25-m intervals for slopes below 23°, 100 m on steeper slopes). Each patch was assigned a single vegetation type: conifer forest, aspen (*Populus tremuloides*), shrub (primarily *Ceanothus cordulatus*), wet meadow (dense grasses and forbs), dry grassland (sparsely vegetated areas dominated by grasses), or unvegetated (exposed rock or sand; Figure 1; see Boisramé, Thompson, Kelly, et al., 2017, for vegetation map details). The model was forced with daily temperature and precipitation data from the Yosemite Headquarters weather station (www.ncdc.noaa.gov; Station ID GHCND:USC00049855). Missing data were gap-filled from the Southern Entrance weather station (www.ncdc.noaa.gov; Station ID GHCND:USC00048380). For the small number of days when no weather data were available, temperature time series were linearly interpolated from preceding and subsequent days, and precipitation was set to 0. A uniform lapse rate was used to spatially interpolate temperature across the domain. We explored whether adopting more complex interpolation techniques, such as those that account for common winter temperature inversions (Dobrowski et al., 2009; Lundquist & Cayan, 2007; Lundquist et al., 2008), would improve the model; however, they did not result in improvements relative to the simple temperature lapse rate (supporting information Text S10).

RHESSys was initialized with a "spin-up" procedure (i.e., running to steady state conditions) using the observed 1969 vegetation cover and calibrated parameters (see section 2.2.2). Fire impacts were represented in the model by imposing litter and biomass removal within mapped fire extents. Fire severity was derived from Landsat data using the relative differenced Normalized Burn Ratio (RdNBR) for post-1983 fires, and a relative difference of the Normalized Difference Vegetation Index (RdNDVI) for earlier fires (Miller & Thode, 2007; Collins et al., 2009; Miller et al., 2016; Morgan et al., 2001). We represented low-severity fires by removing litter layers within the fire perimeter. We removed the litter layer and 50% of biomass to represent moderate-severity fires. Severe fires were modeled by removing all plant biomass and litter layers. Vegetation-type transitions following high-severity fire were determined based on aerial photo records from 1969, 1988, 1997, 2005, and 2012 (Figure 1; Boisramé, Thompson, Kelly, et al., 2017).

Additional details regarding the setup and parameterization of RHESSys for the ICB are given in supporting information Text S4–S11.

2.2.2. Model Calibration and Validation

Calibrated parameters in the model were (i) temperature and precipitation lapse rates, and (ii) multiple subsurface parameters: decay of hydraulic conductivity with depth (m), saturated hydraulic conductivity at the land surface (K), depth of hydrologically active water storage across soil and saprolite layers (sd), the proportion of saturated soil water routed directly (via preferential flow paths) to deeper groundwater stores below plant root access (gw1), and the proportion of these deeper groundwater stores draining to the stream each day (gw2). Subsurface parameters were calibrated against observed streamflow, using information from field observations and other studies (e.g., Clow et al., 2003; Tesfa et al., 2009; Chamorro Lopez, 2016) to set calibration ranges. More calibration details are provided in supporting information Text S10.

Calibration was initially conducted over the entire UMW, allowing us to leverage the streamflow record at Happy Isles. We used a variety of performance metrics and goodness-of-fit measures to calibrate the model to observed streamflow (Table S3). This broad approach to calibration ensured the model captured a range of hydrological processes (Seibert & McDonnell, 2002). The metrics presented in Table S3 included the hydrologic features we expected to reveal the impacts of vegetation change. For example, summer month flows were expected to respond to changing transpiration; February flow volumes, the flow center of mass, and the monthly Nash-Sutcliffe efficiency (NSE) were included to reflect changes to flow timing and basin water storage, and the total annual streamflow volume was included to represent annual water balance. The use of multiple goodness-of-fit metrics including both NSE and Kling-Gupta efficiency (KGE) accounted for the low density of precipitation measurements in the study area. We expected precipitation uncertainty would have large impacts on peak flow predictions, to which NSE is particularly sensitive. Using KGE, which is less sensitive to peak flow than NSE, therefore provides a more robust calibration target (Gupta et al., 2009) by reducing the impact of any "disinformative calibration points" (e.g., streamflow peaks responding to rainfall events that were missed by the observation gage; Beven & Westerberg, 2011; Boyle et al., 2000; Krause et al.,

2005). A total of 4,100 randomly generated parameter combinations were tested in the calibration exercise, of which 296 met the criteria in Table S3.

These 296 parameter sets were tested in an ICB specific model, run for the period 2011–2014 (when clean ICB flow data were available). The ICB rating curve is currently under development, meaning that high flow data are uncertain. The ICB tests therefore considered criteria that are not sensitive to high flows (Table S3). Following this second round of testing, 93 parameter sets were retained and used in all model experiments (Figure S5).

Following calibration, we validated the model to verify that it could do the following:

a. Accurately represent streamflow outside of the calibration period,
b. Capture spatial patterns in snow cover and soil moisture,
c. Realistically represent vegetation growth and water use, and
d. Realistically represent streamflow changes due to fire.

This validation included multiple steps, including the following:

a. Comparing modeled and observed streamflow for years beyond the calibration period using multiple metrics,
b. Comparing the timing of snowmelt to Landsat imagery and comparing modeled soil moisture to field observations,
c. Comparing patch-scale modeled transpiration to results from other models and transpiration measurements in nearby forests (Goulden et al., 2012), and
d. Comparing observed postfire streamflow to models including or omitting fire effects on vegetation.

More details regarding the model calibration and validation are given in supporting information Text S10–S12.

2.3. Model Experiments

We used the calibrated model in two experiments, described below. For all model runs and vegetation cover scenarios, model spin-up simulations were used to initialize RHESSys at steady state vegetation and groundwater conditions.

The first experiment, "historical," modeled the ICB's water balance using the observed, fire-affected, vegetation cover dynamics for water years 1972–2017. The results were compared to a control model run for the same 1972–2017 period but holding 1969 vegetation cover constant. The second model experiment, "extremes," again modeled the ICB using observed weather for 1972–2017, but this time holding vegetation constant at its 2012 condition. This model was also compared to an unburned control which used 1969 vegetation cover. These two vegetation scenarios represent the largest changes in total vegetation cover caused by fire since the restoration of the fire regime (Figure 1). The 2012 vegetation cover appears to still be in a transient state (Boisramé, Thompson, Kelly, et al., 2017) following the change in fire regime, so the results from this model experiment may underestimate the magnitude of water balance changes that could be induced by a natural fire regime in the long run.

Model experiments were run using all calibrated parameter sets (defining subsurface storage and drainage) that met the criteria in Table S3, generating an ensemble of results that we interpreted probabilistically using the generalized likelihood uncertainty estimation method (Beven & Binley, 1992). From this ensemble, we calculated the mean and 95% confidence intervals for all basin-scale model outputs. In each experiment, we asked two questions:

(i) Were the modeled differences in water balance (and water balance components) between burned and unburned scenarios significantly different from 0?
(ii) Given that fire led to significant changes in water balance components, what were the trends, magnitudes, and (in the extremes experiment) climatic sensitivity of these changes?

2.3.1. Model Output

RHESSys can produce exhaustive model output at multiple spatial and temporal scales. Our analysis focused on the major components of the water balance: streamflow volume and timing, ET, subsurface water storage (including both unsaturated and saturated storage), snowpack depth and snowmelt timing, and climatic water deficit (CWD; the difference between potential and actual ET, a measure of how much water stress vegetation is experiencing).

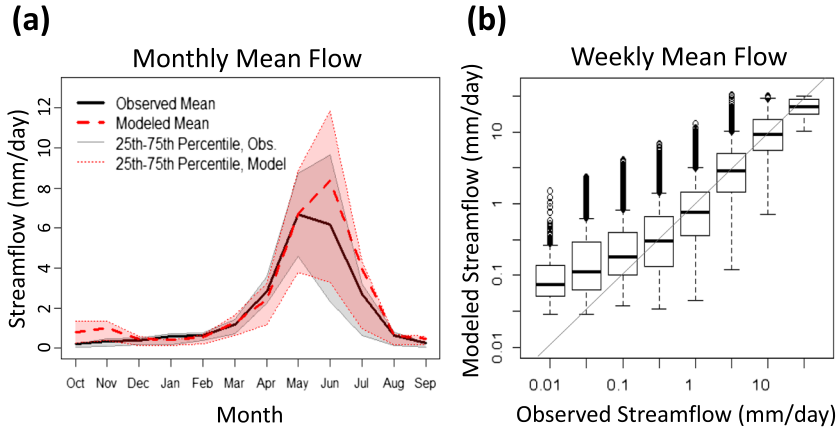

Figure 3. (a) Mean daily flow across all years within each month for both observed UMR flow (black) and modeled UMR flow (red). Shaded areas give the 25th and 75th percentiles of flow in each month across all years. (b) Binned data showing 7-day mean modeled versus observed streamflow on a log scale, compared to a 1:1 line. There is a strong correlation between modeled and observed flows, but the lowest flows are overestimated. The model results shown in both plots are for the parameter set that maximizes Kling-Gupta efficiency of the log of daily streamflow. UMR = Upper Merced River.

We report all volumetric outputs as specific volumes (i.e., volumes per unit watershed area). To isolate changes to areas affected by fire, specific volume changes are reported based on the 92 km^2 located below the highest elevation of any post-1972 fires, rather than the full 150-km^2 basin area. Thus, the magnitudes presented represent the change per unit area of fire-affected watershed. Specific volumes calculated in this manner allow for a more relevant comparison to other watersheds, since different proportions of rocky uplands in different watersheds would greatly affect basin-scale changes due to fire. The omitted 58 km^2 are shown in gray in Figure 2a.

We used a probabilistic approach to assess the meaningfulness of changes between scenarios. For each parameter set, the difference between the results for the two scenarios (e.g., burned versus unburned) was computed. Ninety-five percent confidence intervals were then computed for the ensemble of differences. Differences between scenarios were considered significant if these confidence intervals did not include 0.

3. Results

3.1. Validation

The model's ability to reproduce observed streamflow was first validated by modeling the full UMW for 1966–2015 without including fire effects (Table S5). The model performance was strongest in describing annual streamflow (NSE ≥ 0.88) and monthly streamflow (r^2 ≥ 0.96, NSE ≥ 0.89). Variations in daily time series were also well represented (r^2 ≥ 0.64), although overall model performance at the daily scale was only moderate (KGE ≥ 0.56) and potentially biased by high flows (KGE log(flow) ≥ 0.28 and NSE log(flow) ≥0.55). Late summer flows and the timing of the snowmelt pulse were reproduced well. The model predicted slightly greater variability in streamflow than was observed and tended to overestimate both total and low flows (Figure 3). The model also predicted slightly later peak discharge than observed (Figure 3a). These small inaccuracies are likely due to a combination of imperfect precipitation and temperature input data and our inability to capture certain subsurface flow behavior such as heterogeneous flowpaths through talus (Roy & Hayashi, 2009). Such effects are not dependent on vegetation cover and therefore should not directly impact the model's ability to capture changes due to fire.

Modeled snowmelt timing agreed with satellite imagery, soil moisture spatial patterns were consistent with field observations, and the magnitude of annual transpiration was consistent with observations from experiments in comparable watersheds (supporting information Text S12).

The runoff ratio increased in the burned model scenario, as expected from empirical observations (supporting information Text S12; Boisramé, Thompson, Collins, & Stephens, 2017). However, including fire in the model did not lead to significant improvements in the model's accuracy when reproducing observed streamflow (supporting information Text S12).

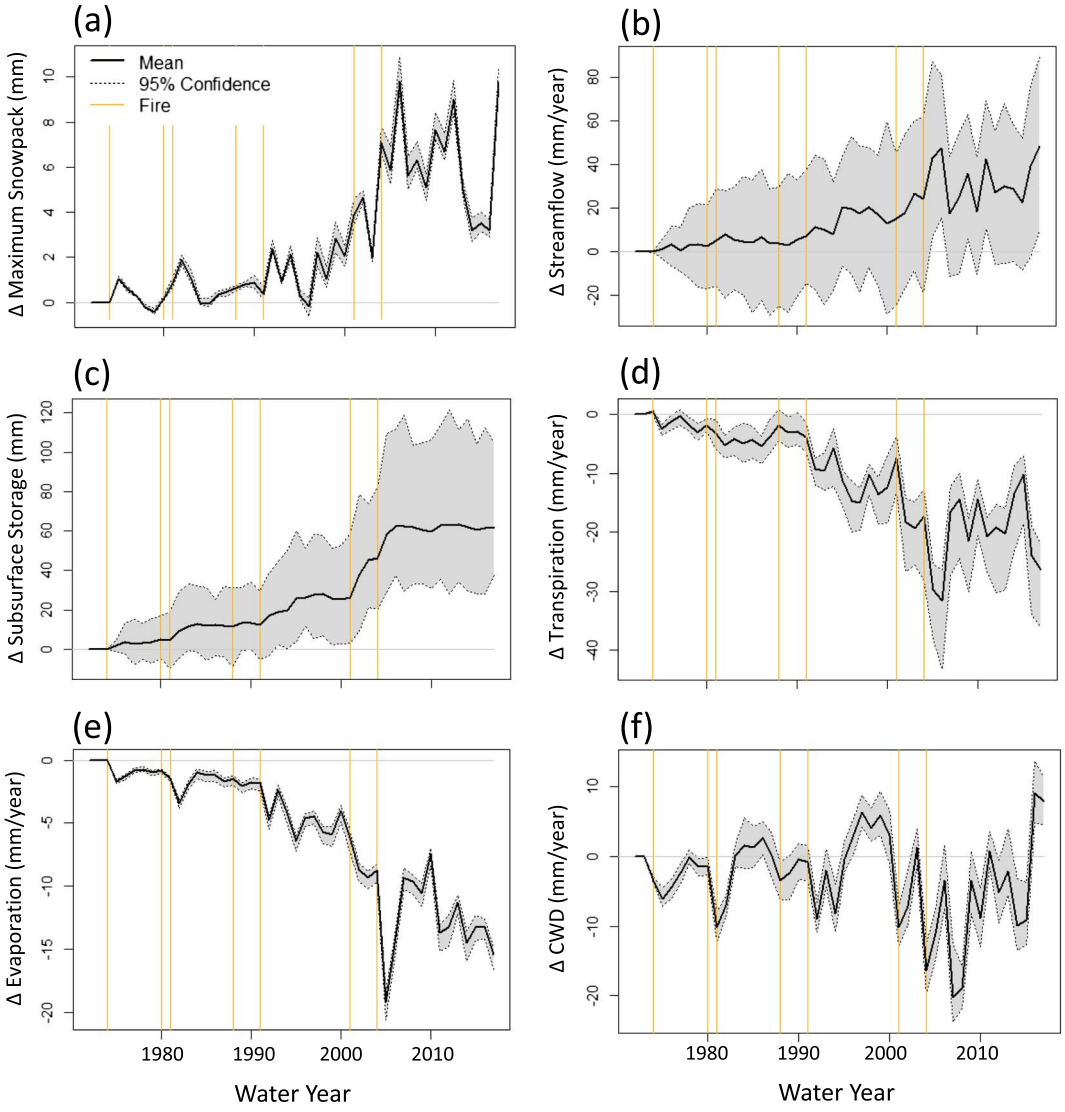

Figure 4. Changes in annual values when fires are included in the model (1972–2017). All changes are calculated for only the portion of the Illilouette Creek Basin affected by fire at some point during the study period. (a) Peak snow water equivalent generally increases over time but is lower in some years, (b) streamflow increases, (c) mean subsurface water storage increases, (d) transpiration generally decreases, (e) evaporation decreases, and (f) climatic water deficit (CWD) decreases following each fire but increases in some regrowth years. Shaded areas show the 95% model confidence interval across the range of subsurface soil parameters. Vertical lines mark the years with the largest fires.

3.2. Model Experiments

3.2.1. Historical Model Experiment

With the restoration of the fire regime from 1972 onward, the model results suggest that over time the ICB became increasingly "wet" relative to the fire-suppressed control. This wet up is indicated by the mean changes in three major water balance elements: first, peak snowpack depths (in terms of snow water equivalent [SWE]) in the burned scenario increased over time relative to the unburned scenario. This effect was generally persistent but varied substantially from year to year, reflecting the importance of interannual variation in climate as a dominant control on fires' hydrologic impacts (Figure 4a). Second, the subsurface water storage in the basin increased persistently during the early part of the new fire regime before stabilizing at approximately 60-mm additional storage by the last decade of the simulation (2008–2017; Figure 4c; note that, for many locations, a higher annual mean subsurface water storage may reflect a lengthening of the time that summer soil moisture remains above a minimum value—e.g., wilting point—for a given location). Third, the enhanced snow and water storage were reflected in a small increase in annual discharge, of

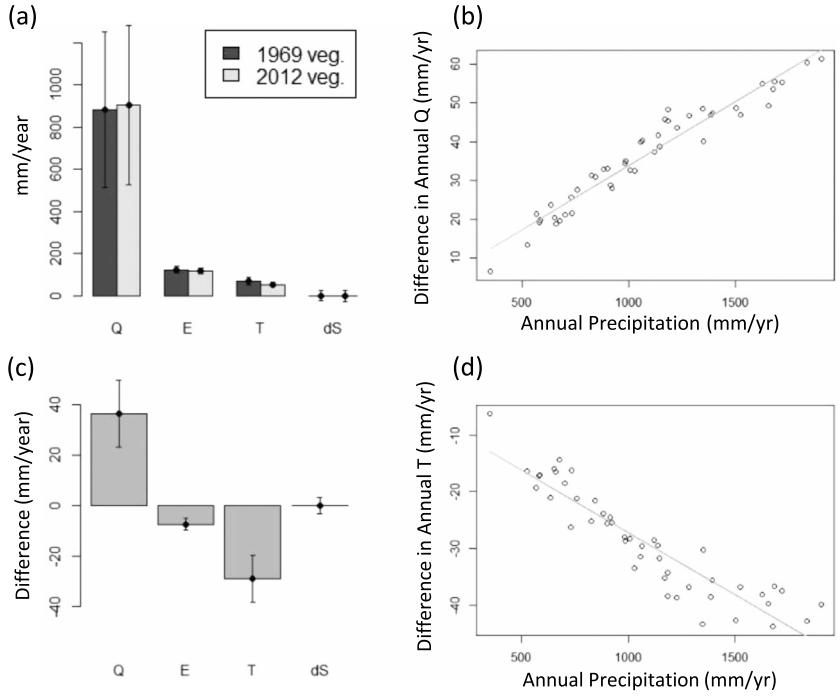

Figure 5. (a) Water balance when using vegetation maps from 1969 (fire-suppressed) and 2012 (after 40 years of fires). The water balance is divided into streamflow (Q), evaporation (E), transpiration (T), and annual change in storage (dS); annual precipitation is equal to the sum of these four components and is the same for both model scenarios. (c) Mean difference between burned and unburned scenarios for each water balance component. Error bars for (a) and (c) denote standard deviation across all years, representing interannual variability. (b) Mean difference between the burned and unburned model scenarios for streamflow compared to each water year's precipitation. (d) Mean difference between the burned and unburned scenarios for transpiration compared to each water year's precipitation. Gray lines show a linear fit to the data. Differences for (b) through (d) were calculated by subtracting results using the 1969 vegetation map from those using the 2012 map.

≈20–40 mm/year for the 2008–2017 period, although the magnitude of the impact varied substantially with model parameters (Figure 4b). While snowpack inputs increased, water losses from the basin via transpiration decreased by 10–30 mm during the last decade of the simulations (Figure 4d). Evaporation decreased following each fire (Figure 4e). Approximately 80% of this decrease was due to less evaporation from canopy surfaces. CWD, a measure of potential water stress experienced by the forests in the ICB, had variable responses but was generally lower in the fire-affected scenarios compared to the control (Figure 4f). All of these variables show their largest and most persistent changes following the wildfires in 2001 and 2004 (Figure 4). These were the most extensive fires experienced in the ICB during the study period (Figure S6) and led to widespread land cover changes that persisted at least until 2012 (the date of the most recent maps; Figure 1).

There is considerable uncertainty regarding the modeled changes in the ICB due to fire. Variations due to the range of calibrated subsurface drainage parameters are particularly notable for subsurface storage and for streamflow responses (Figure 4). The magnitude of effects generally increases with time since 1972 such that changes in transpiration, subsurface water storage, and peak snowpack are significant from 1994 onward. Modeled streamflow changes are only significantly different from 0 for 5 years in the historical simulation. The impact of subsurface parameter uncertainty on the actual magnitude of water balance components (i.e., the range across all parameter sets) is even more extensive, with the range of modeled values often strongly overlapping between the burned and unburned scenarios (supporting information Text S14). In other words, although the magnitude of change evaluated across all parameter sets is often significantly different from 0, the model uncertainty around a given water balance component's magnitude is often larger than the difference between ensemble means for the two scenarios. For this reason, our analysis focused on *differences* between scenarios, rather than focusing on absolute magnitudes expected under each scenario. For comparison, the absolute magnitudes of all modeled values and their uncertainty are shown in the

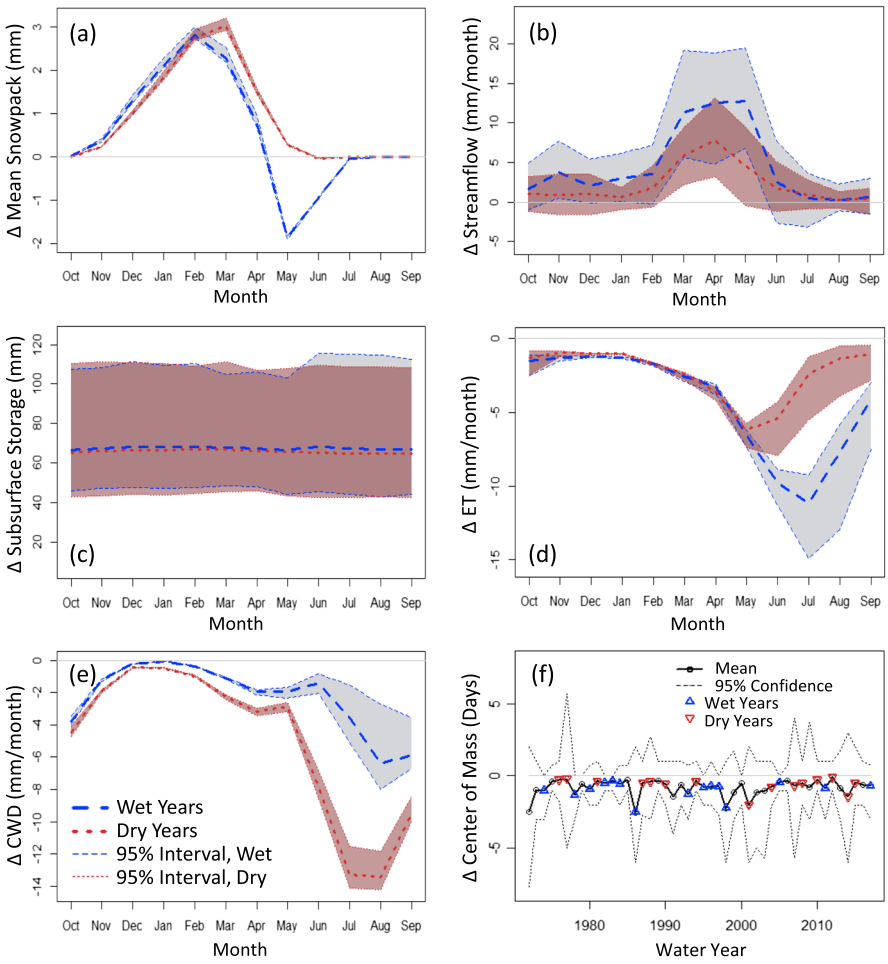

Figure 6. Difference in mean monthly values between model runs using 1969 and 2012 vegetation maps for the top 33% wettest years (blue dashed line) and the bottom 33% driest years (red dotted line) in terms of total water year precipitation (from water years 1972–2017). Shaded areas show the 95% confidence interval for these means, calculated across all model parameterizations. Each Δ value is calculated by subtracting model output using 1969 vegetation from those using 2012 vegetation for the following values: (a) snowpack (b) streamflow, (c) subsurface water storage, (d) evapotranspiration (ET), and (e) climatic water deficit (CWD). (f) Changes in annual center of mass of streamflow timing when using 2012 vegetation map versus 1969 vegetation map; negative values mean that the 2012 vegetation map gives earlier center of mass.

supporting information; annual climatology is also shown to illustrate how climate provides a strong source of interannual variability (Figure S12).

3.2.2. Extremes Model Experiment

In the historical experiment, both weather and vegetation cover varied in time in order to mimic historical conditions as closely as possible. In this experiment we examine the hydrologic responses of landscapes representing two extremes of vegetation condition. Responses are shown across all years in the historic record in order to analyze the impact of weather, separate from any time-dependent changes in vegetation cover. Figure 5 provides an overview of this isolated effect of fire by showing the annual water balance partitioning (between years 1972 and 2017) for fire-suppressed (1969) and contemporary (2012) vegetation cover. A small but significant increase in mean streamflow across all years ($\approx$ 3%) was associated with compensating decreases in evaporation and transpiration ($\approx$ −4% and −25%, respectively). There was large interannual variation in streamflow for both scenarios (standard deviations of 374 and 381 mm for unburned and burned, respectively; Figure 5a; These standard deviations varied only ±5 mm across all model parameterizations), which largely reflects the variable precipitation among the years. Standard deviations in the other annual water balance components are over an order of magnitude smaller than those for streamflow. The differences between scenarios also varied across years, particularly in terms of the partitioning of precipitation

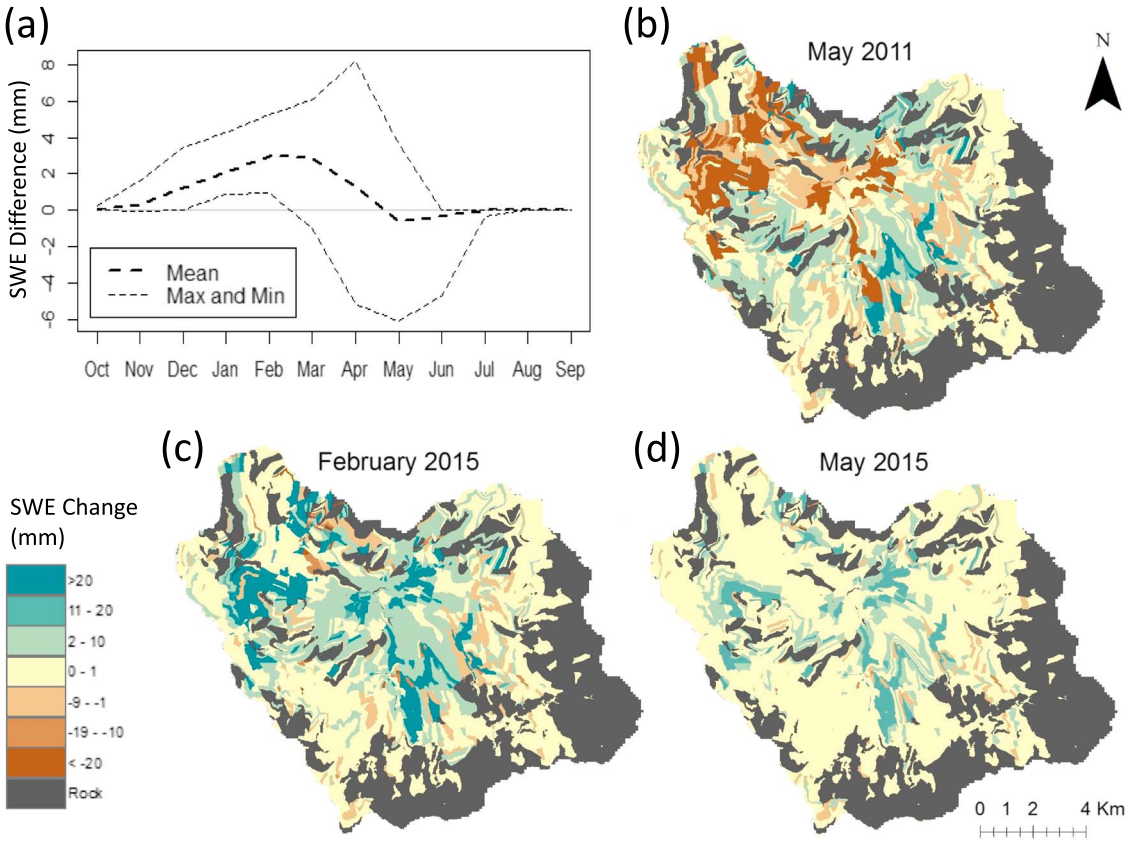

Figure 7. (a) Mean difference in monthly SWE in Illilouette Creek Basin between fire-suppressed (1969) and burned (2012) vegetation covers (a positive value means deeper snowpack using 2012 vegetation compared to 1969 vegetation). Dashed lines show the range between the maximum and minimum changes across all years of weather data (1972–2017). (b–d) Maps of change in SWE for February 2015 and May of 2011 and 2015 when historical fires are included in the model compared to the unburned model scenario. Exposed rock areas which were unaffected by fire are grayed out; nearly all vegetated areas have experienced fire. SWE = snow water equivalent.

between streamflow and transpiration (standard deviations of ≈ 13±3 and 9±1 mm, respectively; Figure 5c). The influence of fire was most pronounced in wet years; precipitation was positively correlated with both the higher flow and lower transpiration in the fire-affected scenario compared to the fire-suppressed scenario (Figures 5b and 5d). This sensitivity indicates that water limitation in dry years reduced the impact of vegetation on modeled water balance. Annual storage was almost constant from year to year, indicating limited carry-over from wet to dry years. Changes in annual water balance components were not strongly related to temperature (not shown). For all values in Figures 5a and 5c, mean variance across all years was greater than mean variance across parameter sets, meaning that natural interannual variability had a stronger impact than model parameter uncertainty.

Peak snowpack depths were greater for the fire-affected vegetation cover, but snowmelt occurred earlier, leading to lower snowpack depths in May and June of wet years (Figure 6a). On average, an additional 3 mm of SWE was present in February (the month with the largest mean increase), which represents an additional 300,000m^3 of water storage in the ICB under fire-affected versus fire-suppressed cover. From October to April the model predicts more snow in the burned versus the unburned model for most years (Figure 7a). This included the exceptionally low snow year of 2015, when even small increases had a large effect proportionally (Figure 7c). The changes in snowpack between burned and unburned scenarios were not spatially uniform, due to differences in elevation, aspect, precipitation, temperature, and their interactions with vegetation changes throughout the basin (Figure 7c). After April the model predicted less SWE on average in burned areas, due to earlier snowmelt (Figure 7a), but these snowpack changes were highly variable through time and space. For example, in May 2011 (a fairly high precipitation year) most burned patches experienced decreases in snow cover compared to the unburned scenario, while in May 2015 (a drought year) fire-induced vegetation change had less overall impact on snowpack but nearly all impacted

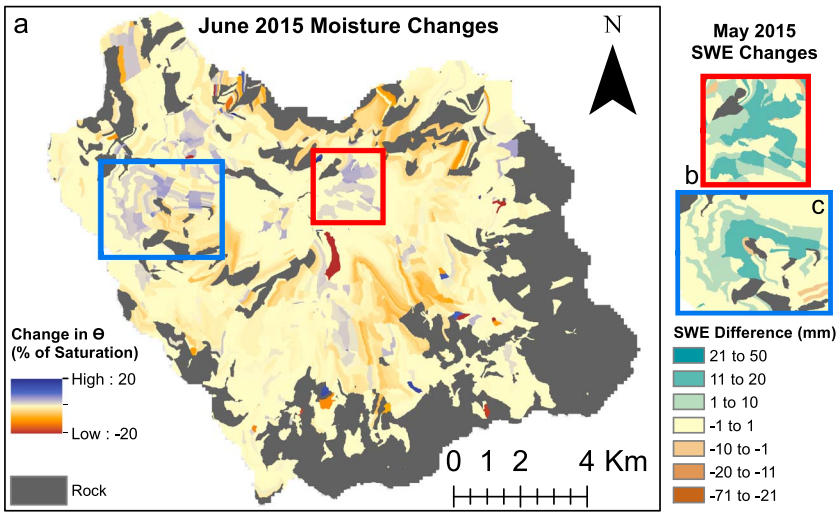

Figure 8. (a) Modeled change in June 2015 soil moisture due to fire between the burned and unburned scenarios, measured using the percent saturation (θ). Blue patches have higher soil moisture when fires are included in the model, and in red patches soil moisture decreases with fire. Red and blue boxes show examples of areas where increased soil moisture is spatially correlated with increased May snowpack, shown in boxes b and c, excerpted from Figure 7d. Exposed rock areas which were unaffected by fire are grayed out; nearly all vegetated areas have experienced fire.

patches showed an increase in SWE (Figures 7b and 7d). Figures 7a, S13, and S16 confirm that in certain years modeled increases in basin-averaged snowpack due to fire can persist until May. This is consistent with empirical observations in the basin which found higher spring SWE in high-severity burn areas (with no remaining tree cover) than in those with forest cover (supporting information Text S12).

The earlier melting of a larger snowpack was reflected in greater March–May streamflow (Figure 6b) and in shifts of up to 19 days earlier for the date of the center of mass of streamflow (Figure 6f). However, most shifts in flow timing due to fire were only a few days, compared to the interannual variability in timing of 72 days, and the change was never significant (Figure 6f). Changes in ET and CWD were concentrated in the months of May–September. Although ET reductions in the fire-affected scenario were greatest in wet years (Figure 6d), CWD reductions were most pronounced in dry years (Figure 6e). There was approximately 60-mm additional water storage in the fire-affected vegetation scenario for all years, with limited seasonality and minimal sensitivity to annual precipitation (Figure 6c). The modeled changes in subsurface water storage were spatially heterogeneous, incorporating both increases and decreases in volumetric water content (Figure 8), which is consistent with field observations made in the basin (Boisramé et al., 2018).

4. Discussion

4.1. Historical Model Experiment

Restoring fire to the ICB resulted in a slow, long-term shift in vegetation cover and composition (Figure 1). The model results presented here indicate that a similarly gradual shift in water balance, toward an overall "wetter" basin, also occurred. With less canopy area in the basin as a whole, peak snowpack water content has increased. The increases resulted mainly from reductions in canopy interception; forest cover removal also reduced longwave radiation emissions from the canopy, which lowered ground snowpack sublimation (Figures S17 and S18; supporting information Text S15). ET decreased, primarily due to reduced transpiration demands and reduced canopy (interception) evaporation. Total subsurface water storage also increased, consistent with observations of increased soil water content in many fire-affected areas throughout the ICB (Boisramé et al., 2018), and with other studies (Brown et al., 2005; He et al., 2013). Although the mean trajectory of change is positive, changes in streamflow are not significantly different from 0 in most modeled years. The fact that changes in streamflow are highly sensitive to parameters that determine subsurface storage and drainage characteristics is important, since Sierran watersheds have substantial spatial heterogeneity in soil and subsurface hydrologic properties (Clow et al., 1996; Tague & Grant, 2009). This may lead to spatially variable patterns of runoff responses to postfire vegetation change. Changes in peak flows and flood risk, often a major negative impact of fire occurrence (Helvey, 1980; Moody & Martin, 2001; Seibert et al., 2010;

Wine & Cadol, 2016), were minimal. However, these risks may be underestimated as ash clogging of soil pores and fire-induced soil hydrophobicity are not represented in the model. The ability to accurately model flood pulses is also limited in general due to the lack of spatially distributed precipitation input data, as precipitation estimates in the Merced River Basin have relatively high uncertainty in terms of both magnitude and spatial patterns (Henn et al., 2018).

Some of the temporal variability in these responses was related to the diverse effects of individual fires, as shown in an example hillslope in supporting information Text S13. Two fires on this hillslope induced only small LAI changes, and consequently there were only small changes in snowpack for a few years following each fire (Figures S11a and S11d). In comparison, a third fire permanently removed a large proportion of LAI, leading to a large and persistent increase in peak snowpack (Figures S11a and S11d). After one fire, the hillslope's outflow increased initially but then decreased below unburned levels 3 years later, while the other two fires led only to flow increases (Figure S11f). These variations show that even within the same relatively small area, different fires can have varying impacts.

Fire impacts snow accumulation and melt by thinning canopies or replacing forest cover with shorter and less dense vegetation types. These reductions in LAI reduce snow interception, which in turn reduces interception sublimation and melt (Lundberg & Halldin, 2001; Svoma, 2017; Figure S17). Reduced LAI also increases shortwave radiation while decreasing longwave radiation incident on the ground snowpack (Lundquist et al., 2013; Svoma, 2017). The net effect of reduced interception, increased shortwave, and decreased longwave radiation on the snowpack depends on the relative importance of all three processes. This relative importance varies with air temperature, solar radiation, and the amount and timing of snowfall. Snowfall and temperature vary both interannually and spatially and interact with the spatial pattern of fire effects on vegetation. Changing canopy cover also alters wind speed and other conductance terms at the surface, influencing sublimation.

All of these interacting processes lead to considerable spatiotemporal variability in snowpack response, as is illustrated by comparing modelled changes in May snowpack from fire-suppressed to fire-affected conditions in 2011 and 2015 (Figures 7b and 7d). Fire-affected patches show both increases and decreases in SWE for 2011, while in 2015 fire-affected patches mostly show higher SWE. This difference arises from a combination of drought conditions and warmer 2015 temperatures, as well as different distributions of snow cover (e.g., in May 2015 the lowest elevations have no remaining snow available to be impacted by vegetation one way or another, while in May 2011 the low-elevation snow is mostly melting faster under the burned scenario). Modeled spring snowpack is lower when increased solar radiation causes accelerated spring melting and is higher when the lowered longwave radiation from the canopy outweighs the raised shortwave solar radiation (which occurs mostly in warmer years; Figure S15; Lundquist et al., 2013). These model results suggest that open burned patches were particularly important for snowpack retention during hot, dry years. More fundamentally, the spatial and temporal variability in the responses highlights the potential pitfalls of attempting to extrapolate from small-scale or immediate postfire observations to predict the long-term, basin-scale impacts of fire regime change. Further, the longer-term effects are likely to vary as a function of the severity of fire and climate trajectory following the fire.

We also note that RHESSys likely underestimates the spatial heterogeneity in the ICB. RHESSys is a lumped canopy model which simplifies the relationship between fire-related change in canopy structure and the resulting changes in snowpack radiation fluxes as well as near-surface aerodynamic conductance. A model that explicitly accounts for fine-scale heterogeneity in canopy structure, including the distributions of gaps and individual trees, would be likely to add even more heterogeneity to estimates of snowpack responses to fire.

The fire-affected model showed lower CWD than the model without fire for most years (Figure 4f). This suggests that enhanced dry-year snowpack in conjunction with overall increases in subsurface water availability in the ICB resulted in more resilient forest cover. These CWD reductions were present during the extreme drought years of 2012–2015, even though there had not been any major fires in the ICB since 2004 (Figure 4f), and are consistent with observations of reduced tree mortality in the ICB compared to nearby watersheds during the drought summers of 2014 and 2015 (Boisramé et al., 2017) and other studies showing decreases in drought stress and mortality following forest thinning (e.g., Grant et al., 2013; Hood et al., 2016; Tague et al., 2019).

Previous studies of the ICB showed that the landscape does not appear to have reached a steady state, and that land cover metrics are trending toward more heterogeneity and less forest cover as wildfires and regrowth continue to alter the watershed (Boisramé, Thompson, Kelly, et al., 2017). This suggests that the observed and modeled changes to the hydrologic cycle in this basin over the past 45 years do not represent the maximum amount of change possible; continued burning could lead to more changes along the trends observed in Figure 4, although climate change might mediate some of these changes.

4.2. Extremes Model Experiment

The extremes model experiment highlighted the interaction of climate with vegetation in generating a range of water balance responses to fire impacts on the ICB. Results indicated a first-order impact of climate on streamflow (interannual standard deviation of ≈ 400 mm) which was largely independent of vegetation cover (standard deviations were similar regardless of vegetation). A second-order effect of vegetation cover on water balance partitioning between ET and streamflow was also sensitive to climate—with the vegetation impacts largest in wet years (Figures 5d, 6b, and 6d). This is consistent with other Sierra Nevada studies that indicate ET reduction due to thinning is greatest in wet environments (Roche et al., 2018). Streamflow impacts were greatest during spring, while summer baseflow was insensitive to vegetation change (Figure 6b), suggesting water-limited conditions in summer, regardless of changes in vegetation cover. Lower CWD in the burned scenario (especially during summer in the driest years) shows that fires may support greater forest health by increasing plant water availability during times of water stress (Figure 6e). Thus, the benefits of increased water availability are primarily expressed through reduced vegetation water stress rather than changes in summer baseflow.

Effects on soil moisture did not vary greatly between wet and dry years or between seasons (Figure 6c), potentially because subsurface water storage responds more slowly to change than do other hydrologic variables. Soil moisture changes were highly spatially variable, and localized areas of increased moisture appear to be correlated with areas of increased spring snowpack (Figure 8). Such areas can be important hydrologic refugia, mitigating the effects of droughts or a warming climate (McLaughlin et al., 2017).

Spring snowpack was either lower or higher in the burned scenario, depending on the balance between higher snowmelt and lower losses from sublimation and interception melt at the basin scale (Figure S17). The largest impacts of fire were to lessen the amount of snow sublimated from the canopy while causing greater melt from the snowpack on an annual scale (Figure S17). Higher melt is largely due to having a deeper peak snowpack available for melting but also partly due to more solar radiation reaching the snowpack during warm spring periods (results not shown). Lower sublimation and melting of intercepted snowpack were due to less snow being intercepted when LAI was reduced. The burned scenario also showed slightly lower basin-averaged sublimation from snowpack on the ground, which was associated with a decline in longwave radiation with canopy reduction (supporting information Text S15). Changes in snowpack sublimation, however, were small (≈1 mm/year when averaged over the watershed) and highly variable in space and time. These results are consistent with the modeling results of Svoma (2017), which showed basin-scale decreases in sublimation in response to reduced LAI in an Arizona watershed, with snowpack sublimation decreasing to a much lesser extent than canopy sublimation.

Modeled increases in spring snowpack during dry years (Figures 6a, 7d, S16, and S17) as well as decreased water stress during dry years (Figure 6e) suggest that natural wildfire regimes could help protect watersheds from predicted increases in drought severity and reductions in snowpack under climate change (Tague & Dugger, 2010; Maurer, 2007). However, these results also suggest that observed streamflow increases in the past (Boisramé et al., 2017) may not continue into the future if the climate is drier (Figure 5b), though climate models disagree on the net impact of climate change on California's annual precipitation (Maurer, 2007).

Despite changes to spring snowpack and subsurface water storage, the models did not show a consistent impact of fire on streamflow timing (Figure 6f). This may be largely due to snowmelt from higher, rocky areas (which are unaffected by fire) being the dominant control on streamflow timing. However, deeper peak snowpacks (due to reduced interception and reduced longwave radiation from vegetation) coupled with increased basin-averaged melting of spring snowpack (due to increased sun exposure) led to significantly higher streamflows during the spring snowmelt periods (Figures 6a and 6b). This also demonstrates the importance of snowpack depth in driving increases in streamflow. Across all model parameterizations, spring runoff was higher under 2012 (burned) vegetation. This could counter predicted reductions in stream-

flow in warmer climates, which are expected to happen as snowpacks melt more slowly, earlier in the year (Barnhart et al., 2016; Trujillo & Molotch, 2014). In fact, a previous study showed runoff ratios decreasing in nearby unburned watersheds, while the UMR runoff ratio stayed steady or increased slightly, so the restored fire regime may already be countering effects of climate change (Boisramé et al., 2017). This timing of streamflow increases has important implications for reservoirs and water-dependent ecosystems downstream.

4.3. Model Performance and Limitations

Our models are unique in that they represent observed landscape changes due to fire over multiple decades. This provides the opportunity to estimate actual changes in hydrological partitioning that have occurred and to verify some of these estimates. We expected model output from the burned scenario to better match observed streamflow, since the burned scenario should be closer to the true land cover dynamics in the study watersheds. However, this was not always the case due to the fact that the model has a slight positive bias rather than completely random error. The differences in streamflow (and thus in measures of accuracy) between the historical and unburned runs were very small, which is at least partially due to UMW and ICB's high proportion of exposed bedrock, and therefore is not susceptible to change from wildfire. Some measures of model accuracy, especially those that incorporate timing of streamflow such as monthly flow correlation and date of center of mass, showed slightly higher model accuracy when fire was included (although this increase in accuracy was not statistically significant). It is expected that streamflow timing would be altered by fire due to vegetation cover's effects on snowpack (Godsey et al., 2014). Observations of increased runoff ratio and soil moisture appear to match with model output, suggesting that at least coarse effects of fire on this watershed are being well represented.

While our models capture fire-induced landscape changes fairly realistically by incorporating maps of actual vegetation cover over time and modeling the resulting changes in LAI, they also include some simplifications of hydrologically relevant processes. For example, high-severity fire was modeled as removing all vegetation and litter cover, although in practice this is rarely achieved; this could have led to overestimates of reductions in interception, transpiration, and evaporation from litter surfaces. Changes to forest structure, especially gap sizes, could be important to snow dynamics (Lawler & Link, 2011; Stevens, 2017). However, such effects were not fully captured in this model since we represented thinning with a proportional stand-scale reduction in biomass, litter, and LAI rather than modeling specific changes in gap sizes, or tree height and stem size. This simplification potentially underestimates the impact of increased turbulent water vapor fluxes in forest gaps. The model also simplifies the relationship between rooting depth, shallow soil moisture, and soil evaporation; this could lead to slight overestimation of evaporation reductions following fire (supporting information Text S14). In addition, there are effects of fires other than vegetation/litter removal that are not captured in the model, such as reduced albedo from charred surfaces (Burles & Boon, 2011; Gleason et al., 2013; Gleason et al., 2019), potentially reduced soil infiltration capacity (Neary et al., 2005), or increased erosion (e.g., Helvey, 1980). If they could have been included, these processes might have led to increased surface runoff and reduced groundwater recharge in the burned model scenario and had various counteractive impacts on snow dynamics and evaporation. However, most of these effects are likely to be more important in the short term following fire, while the focus of this study is on longer-term effects of vegetation cover change. Also, compared to large-scale vegetation change, the omitted processes are likely to have secondary effects on water balance partitioning and partially compensate for each other.

Although the model results match observations of higher peak snowpack in burned areas of the ICB, modeled late spring snowpack dynamics did not always match observations (supporting information Text S12). As noted above, there are a number of limitations to RHESSys estimates. Most importantly, RHESSys estimates do not account for the spatial arrangement of canopy gaps, which likely affect the impact of tree-scale longwave radiation on snowmelt as well as the response of wind and aerodynamic conductance to changes in canopy structure with fire. Further, uncertainty in surface temperatures, which have a dramatic impact on longwave estimates (which are proportional to temperature to the fourth power), may also contribute substantial error to estimates of spring snowpack losses. Further study should explore how to better account for the impact of finer-scale canopy structural parameters on RHESSys energy and moisture estimates.

Although both Figures 4a and 6a show very narrow confidence intervals for fire effects on snowpack, these intervals reflect only uncertainties in the model's subsurface parameters (which affect snowpack only

through small variations in LAI), not uncertainty in precipitation inputs, although the precipitation inputs have fairly high uncertainty (Henn et al., 2018). The sensitivity of snowpack responses to precipitation inputs (Figure 6a) shows that errors in precipitation data could have meaningful impacts on the model output. However, the general trend of higher peak snowpack appears to be robust across the range of precipitation inputs used, giving us high confidence in the direction of change even if the full range of uncertainty is not captured.

5. Conclusion

The reintroduction of a near-natural wildfire regime to the ICB has reduced transpiration, increased peak snowpack while leading to earlier snowmelt overall, increased subsurface water storage in the basin, and is likely to have increased streamflow. The changes are suggestive of a slight shift in hydrological regime from a more arid, densely forested basin, to a more mesic basin, in which vegetation fragmentation reduces losses of water to the atmosphere and increases water storage and discharge from the landscape. This shift is sustained by fire: Were fire to be removed from the basin again, it is probable that woody cover and water use would again increase. The hydrological impact of the changed fire regime is thus broadly positive. From a cost-benefit perspective, it suggests that there are probable (although uncertain and highly variable with climate) increases in snowpack and streamflow: up to 1% higher, or 5×10^5 m^3 of additional SWE per year, and up to 7×10^6 m^3 of increased streamflow per year (approximately 1/60 of the capacity of the nearby Hetch-Hetchy reservoir and 1/10 of mean flow from the fire-affected portion of the watershed), with no indication of significant increases in flood risk. While these differences may provide an important increased water store, they can be relatively small compared to the watershed's total output (7×10^6 m^3 is approximately 5% of mean annual outflow from the ICB)—and thus even significant changes may not always be apparent in observed data given high interannual variation in these water fluxes. For this watershed, comparing UMR streamflow records to reference (unburned) watersheds does reveal a likely increase in streamflow due to fire, also on the order of 5% (Boisramé et al., 2017). Other studies of changing forest structure on streamflow, however, have shown a wide range of impacts including increases (again approximately 5%; Roche et al., 2018, negligible changes ; Biederman et al., 2014) and even decreases (e.g., Adams et al., 2012) due to compensating changes in evaporation and other factors. The small-magnitude, high interannual variation and sensitivity to drainage parameters of the impacts of fire-mediated vegetation change shown here suggests why changes to streamflow may be both hard to detect and vary with location and climate.

Increases in subsurface water storage and reductions in transpiration were predicted by all model runs and resulted in reductions in climatic water stress that were also predicted by all models for several important drought periods. Thus, how these changes should be evaluated in the context of setting policy for forest management in the western United States remains uncertain, but the model results are broadly consistent with a possible “win-win-win” scenario in which the managed wildfire regime of ICB yields benefits for water management, forest health, and reductions in fire hazard (Boisramé et al., 2017).

The model results presented here contain nontrivial uncertainties, due to parameter uncertainty and the simplifications of snowpack dynamics, fire-related changes to vegetation and soils, and other process representations in RHESSys. However, the overall trends in hydrologic variables appear to be consistent across a range of parameters, and the larger-scale effects of fire should be well captured. Future efforts should address more comprehensive model representation of fire impacts, drawing on new observations made with lidar (for example) to describe changes in forest density, representing species changes and understory changes in more detail, exploring likely postfire soil modifications in western U.S. mountains, and quantifying the role of burned surfaces on snowpack energy dynamics. Addressing whether climate change will amplify or reduce the hydrological impacts of vegetation change is another important area for future study, as our results show that hydrologic impacts vary with temperature and precipitation. For example, fires led to increased spring snowpack in years with low snowpack, and snowpack is expected to decrease due to climate change (Maurer, 2007). While preliminary, with its focus on a single basin, the example of the ICB is encouraging. It suggests fire management could have important benefits for the natural infrastructure provided by mountain watersheds in the western United States. While the local changes in water balance are modest, they have potential for extensive upscaling, and to deliver benefits in areas of significant stress: water supply, forest health, and fire risk.

Acknowledgments
Model input and output files are available at the website (http://www.hydroshare.org/resource/ed929a241cda4a76a3730772a4fe7555). Model parameters are described in the supporting information accompanying this manuscript. Data used for this manuscript include the following: vegetation maps created by the authors (https://doi.org/10.1016/j.foreco.2017.07.034); 1997 Yosemite National Park vegetation map (https://irma.nps.gov); Merced River flow data (https://nwis.waterdata.usgs.gov/nwis/uv/?site_no=11264500&agency_cd=USGS&referred_module=sw); Illilouette Creek flow data (https://irma.nps.gov/AQWebPortal/Data/Location/Summary/Location/YOSE_MERC_ILLI); weather data from multiple stations named in the text (http://cdec.water.ca.gov and www.ncdc.noaa.gov); and fire perimeters (http://frap.fire.ca.gov/data/frapgisdata-sw-fireperimeters_download). Thank you to Kate Wilkin, Brandon Collins, Jim Roche, and Jan van Wagtendonk for sharing their expertise on wildfire and hydrology in the ICB. Also, thank you to all field crew members and volunteers: Miguel Naranjo, Andy Wong, Perth Silvers, Jeremy Balch, Seth Bergeson, Amanda Atkinson, Tom Bruton, Diane Taylor, Madeleine Jensen, Isabel Schroeter, Katy Abbott, Bryce King, Zubair Dar, Katherine Eve, Sally McConchie, Karen Klonsky, Yves Boisramé, James Hart, Caroline Delaire, Louis Alexandre-Couston, Catherine Fong, Melissa Thaw, Anthony Everhart, Skye Niles, Lena Nitsan, Chris Phillips, Anthony Ambrose, Wendy Baxter, Jens Stevens, Stacey Sargent Frederick, and Kirt Siders, as well as lab assistants Julia Cavalli, Melissa Ferriter, Kelly Archer, Frank He, and Jordan French. Thank you to Tyler Brandt for suggestions regarding precipitation modeling and Erin Hanan for providing some of the vegetation parameterizations. Financial assistance for this project was provided by Joint Fire Sciences, the University of California Agricultural and Natural Resources Grants Program, Sigma Xi Grant in Aid of Research, the UC Berkeley SMART program, and the UC Berkeley Philomathia Graduate Fellowship in Environmental Sciences. We especially thank Yosemite National Park for allowing us to take measurements in wilderness areas and the Yosemite Resources Management and Science Division for collecting and sharing the gage data for Illilouette Creek.

References

Adams, H. D., Luce, C. H., Breshears, D. D., Allen, C. D., Weiler, M., Hale, V. C., et al. (2012). Ecohydrological consequences of drought- and infestation- triggered tree die-off: Insights and hypotheses. *Ecohydrology*, *5*(2), 145–159. https://doi.org/10.1002/eco.233

Andreadis, K. M., Storck, P., & Lettenmaier, D. P. (2009). Modeling snow accumulation and ablation processes in forested environments. *Water Resources Research*, *45*, W05429. https://doi.org/10.1029/2008WR007042

Bair, E. H., Dozier, J., Davis, R. E., Colee, M. T., & Claffey, K. J. (2015). Cues—A study site for measuring snowpack energy balance in the Sierra Nevada. *Frontiers in Earth Science*, *3*, 58. https://doi.org/10.3389/feart.2015.00058

Bales, R. C., Goulden, M. L., Hunsaker, C. T., Conklin, M. H., Hartsough, P. C., O'Geen, A. T., et al. (2018). Mechanisms controlling the impact of multi-year drought on mountain hydrology. *Scientific Reports*, *8*(1), 690. https://doi.org/10.1038/s41598-017-19007-0

Barnhart, T. B., Molotch, N. P., Livneh, B., Harpold, A. A., Knowles, J. F., & Schneider, D. (2016). Snowmelt rate dictates streamflow. *Geophysical Research Letters*, *43*, 8006–8016. https://doi.org/10.1002/2016GL069690

Bart, R. R., Tague, C. L., & Moritz, M. A. (2016). Effect of tree-to-shrub type conversion in lower montane forests of the Sierra Nevada (USA) on streamflow. *PLOS ONE*, *11*(8), e0161805. https://doi.org/10.1371/journal.pone.0161805

Beven, K., & Binley, A. (1992). The future of distributed models: Model calibration and uncertainty prediction. *Hydrological Processes*, *6*(3), 279–298. https://doi.org/10.1002/hyp.3360060305

Beven, K., & Westerberg, I. (2011). On red herrings and real herrings: Disinformation and information in hydrological inference. *Hydrological Processes*, *25*(10), 1676–1680. https://doi.org/10.1002/hyp.7963

Biederman, J. A., Harpold, A. A., Gochis, D. J., Ewers, B. E., Reed, D. E., Papuga, S. A., & Brooks, P. D. (2014). Increased evaporation following widespread tree mortality limits streamflow response. *Water Resources Research*, *50*, 5395–5409. https://doi.org/10.1002/2013WR014994

Bladon, K. D., Emelko, M. B., Silins, U., & Stone, M. (2014). Wildfire and the future of water supply. *Environmental Science and Technology*, *48*(16), 8936–8943. https://doi.org/10.1021/es500130g

Boisramé, G. F., Thompson, S., Collins, B., & Stephens, S. (2017). Managed wildfire effects on forest resilience and water in the Sierra Nevada. *Ecosystems*, *20*(4), 717–732. https://doi.org/10.1007/s10021-016-0048-1

Boisramé, G. F., Thompson, S. E., Kelly, M., Cavalli, J., Wilkin, K. M., & Stephens, S. L. (2017). Vegetation change during 40 years of repeated managed wildfires in the Sierra Nevada, California. *Forest Ecology and Management*, *402*, 241–252. https://doi.org/10.1016/j.foreco.2017.07.034

Boisramé, G. F., Thompson, S. E., & Stephens, S. L. (2018). Hydrologic responses to restored wildfire regimes revealed by soil moisture-vegetation relationships. *Advances in Water Resources*, *112*, 124–146. https://doi.org/10.1016/j.advwatres.2017.12.009

Boyle, D. P., Gupta, H. V., & Sorooshian, S. (2000). Toward improved calibration of hydrologic models: Combining the strengths of manual and automatic methods. *Water Resources Research*, *36*, 3663–3674. https://doi.org/10.1029/2000WR900207

Brown, A. E., Zhang, L., McMahon, T. A., Western, A. W., & Vertessy, R. A. (2005). A review of paired catchment studies for determining changes in water yield resulting from alterations in vegetation. *Journal of Hydrology*, *310*(1–4), 28–61. https://doi.org/10.1016/j.jhydrol.2004.12.010

Burles, K., & Boon, S. (2011). Snowmelt energy balance in a burned forest plot, Crowsnest Pass, Alberta, Canada. *Hydrological Processes*, *25*(19), 3012–3029. https://doi.org/10.1002/hyp.8067

Chamorro Lopez, A. O. (2016). Prediction of the variability of soil depth using qualitative and quantitative geomorphological information Information: Sierra Nevada, CA, USA. Doctoral dissertation, Texas A&M University. Retrieved from http://hdl.handle.net/1969.1/156956

Christensen, L., Tague, C. L., & Baron, J. S. (2008). Spatial patterns of simulated transpiration response to climate variability in a snow dominated mountain ecosystem. *Hydrological Processes*, *22*(18), 3576–3588.

Clow, D. W., Mast, M. A., & Campbell, D. H. (1996). Controls on surface water chemistry in the Upper Merced River Basin, Yosemite National Park, California. *Hydrological Processes*, *10*(5), 727–746. https://doi.org/10.1002/(SICI)1099-1085(199605)10:5h727::AID-HYP316i3.0.CO;2-D

Clow, D. W., Schrott, L., Webb, R., Campbell, D. H., Torizzo, A., & Dornblaser, M. (2003). Ground water occurrence and contributions to streamflow in an alpine catchment, Colorado Front Range. *Groundwater*, *41*(7), 937–950. https://doi.org/10.1111/j.1745-6584.2003.tb02436.x

Collins, B. M., Everett, R. G., & Stephens, S. L. (2011). Impacts of fire exclusion and recent managed fire on forest structure in old growth Sierra Nevada mixed-conifer forests. *Ecosphere*, *2*(4), 1–14. https://doi.org/10.1890/ES11-00026.1

Collins, B. M., Kelly, M., van Wagtendonk, J. W., & Stephens, S. L. (2007). Spatial patterns of large natural fires in Sierra Nevada wilderness areas. *Landscape Ecology*, *22*(4), 545–557. https://doi.org/10.1007/s10980-006-9047-5

Collins, B. M., Lydersen, J. M., Fry, D. L., Wilkin, K., Moody, T., & Stephens, S. L. (2016). Variability in vegetation and surface fuels across mixed-conifer-dominated landscapes with over 40 years of natural fire. *Forest Ecology and Management*, *381*, 74–83. https://doi.org/10.1016/j.foreco.2016.09.010

Collins, B. M., Miller, J. D., Thode, A. E., Kelly, M., van Wagtendonk, J. W., & Stephens, S. L. (2009). Interactions among wildland fires in a long-established Sierra Nevada natural fire area. *Ecosystems*, *12*(1), 114–128. https://doi.org/10.1007/s10021-008-9211-7

Collins, B. M., & Stephens, S. L. (2007). Managing natural wildfires in Sierra Nevada wilderness areas. *Frontiers in Ecology and the Environment*, *5*(10), 523–527. https://doi.org/10.1890/070007

Collins, B. M., & Stephens, S. L. (2010). Stand-replacing patches within a 'mixed severity' fire regime: Quantitative characterization using recent fires in a long-established natural fire area. *Landscape Ecology*, *25*(6), 927–939. https://doi.org/10.1007/s10980-010-9470-5

Department of Water Resources (2008). Managing an uncertain future: Climate change adaptation strategies for California's water: State of California Resources Agency. www.water.ca.gov/climatechange/docs/ClimateChangeWhitePaper.pdf.

Dettinger, M. D., Cayan, D. R., Meyer, M. K., & Jeton, A. E. (2004). Simulated hydrologic responses to climate variations and change in the Merced, Carson, and American River Basins, Sierra Nevada, California, 1900–2099. *Climatic Change*, *62*(1-3), 283–317. https://doi.org/10.1023/B:CLIM.0000013683.13346.4f

Dobrowski, S. Z., Abatzoglou, J. T., Greenberg, J. A., & Schladow, S. G. (2009). How much influence does landscape-scale physiography have on air temperature in a mountain environment? *Agricultural and Forest Meteorology*, *149*(10), 1751–1758. https://doi.org/10.1016/j.agrformet.2009.06.006

Dugger, A. L., Tague, C., Allen, C. D., & Ringler, T. (2013). Which mechanisms dominate the net effects of forest thinning on water yield and forest productivity in the semi-arid Santa Fe Municipal Watershed? In *Abstract GC11B-0981 presented at 2013, Fall Meeting*, AGU, San Francisco, CA, pp. 9–13. Retrieved from http://abstractsearch.agu.org/meetings/2013/FM/GC11B-0981.html.

Ellis, C. R., Pomeroy, J. W., & Link, T. E. (2013). Modeling increases in snowmelt yield and desynchronization resulting from forest gap-thinning treatments in a northern mountain headwater basin. *Water Resources Research*, *49*, 936–949. https://doi.org/10.1002/wrcr.20089

Frank, J. M., Massman, W. J., Ewers, B. E., & Williams, D. G. (2019). Bayesian analyses of 17 winters of water vapor fluxes show bark beetles reduce sublimation. *Water Resources Research*, *55*, 1598–1623. https://doi.org/10.1029/2018WR023054

Gleason, K. E., McConnell, J. R., Arienzo, M. M., Chellman, N., & Calvin, W. M. (2019). Four-fold increase in solar forcing on snow in western U.S. burned forests since 1999. *Nature Communications*, *10*, 2026. https://doi.org/10.1038/s41467-019-09935-y

Gleason, K. E., Nolin, A. W., & Roth, T. R. (2013). Charred forests increase snowmelt: Effects of burned woody debris and incoming solar radiation on snow ablation. *Geophysical Research Letters*, *40*, 4654–4661. https://doi.org/10.1002/grl.50896

Godsey, S. E., Kirchner, J. W., & Tague, C. L. (2014). Effects of changes in winter snowpacks on summer low flows: Case studies in the Sierra Nevada, California, USA. *Hydrological Processes*, *28*(19), 5048–5064. https://doi.org/10.1002/hyp.9943

Goulden, M. L., Anderson, R. G., Bales, R. C., Kelly, A. E., Meadows, M., & Winston, G. C. (2012). Evapotranspiration along an elevation gradient in California's Sierra Nevada. *Journal of Geophysical Research*, *117*, G03028. https://doi.org/10.1029/2012JG002027

Grant, G. E., Tague, C. L., & Allen, C. D. (2013). Watering the forest for the trees: An emerging priority for managing water in forest landscapes. *Frontiers in Ecology and the Environment*, *11*(6), 314–321. https://doi.org/10.1890/120209

Green, W. H., & Ampt, G. A. (1911). Studies on soil physics. *The Journal of Agricultural Science*, *4*(1), 1–24. https://doi.org/10.1017/S0021859600001441

Gupta, H. V., Kling, H., Yilmaz, K. K., & Martinez, G. F. (2009). Decomposition of the mean squared error and NSE performance criteria: Implications for improving hydrological modelling. *Journal of Hydrology*, *377*(1–2), 80–91. https://doi.org/10.1016/j.jhydrol.2009.08.003

He, L., Ivanov, V. Y., Bohrer, G., Thomsen, J. E., Vogel, C. S., & Moghaddam, M. (2013). Temporal dynamics of soil moisture in a northern temperate mixed successional forest after a prescribed intermediate disturbance. *Agricultural and Forest Meteorology*, *180*, 22–33. https://doi.org/10.1016/j.agrformet.2013.04.014

Helvey, J. D. (1980). Effects of a north central Washington wildfire on runoff and sediment production. *Water Resources Bulletin*, *16*, 627–634.

Henn, B., Clark, M. P., Kavetski, D., Newman, A. J., Hughes, M., McGurk, B., & Lundquist, J. D. (2018). Spatiotemporal patterns of precipitation inferred from streamflow observations across the Sierra Nevada mountain range. *Journal of Hydrology*, *556*, 993–1012. https://doi.org/10.1016/j.jhydrol.2016.08.009

Hood, S. M., Baker, S., & Sala, A. (2016). Fortifying the forest: Thinning and burning increase resistance to a bark beetle outbreak and promote forest resilience. *Ecological Applications*, *26*(7), 1984–2000. https://doi.org/10.1002/eap.1363

Kane, V. R., Lutz, J. A., Alina Cansler, C., Povak, N. A., Churchill, D. J., Smith, D. F., et al. (2015). Water balance and topography predict fire and forest structure patterns. *Forest Ecology and Management*, *338*, 1–13. https://doi.org/10.1016/j.foreco.2014.10.038

Kattelmann, R. C., Berg, N. H., & Rector, J. (1983). The potential for increasing streamflow from Sierra Nevada watersheds. *JAWRA Journal of the American Water Resources Association*, *19*(3), 395–402. https://doi.org/10.1111/j.1752-1688.1983.tb04596.x

Krause, P., Boyle, D. P., & Bäse, F. (2005). Comparison of different efficiency criteria for hydrological model assessment. *Advances in Geosciences*, *5*, 89–97. https://doi.org/10.5194/adgeo-5-89-2005

Lane, P. N. J., Feikema, P. M., Sherwin, C. B., Peel, M. C., & Freebairn, A. C. (2010). Modelling the long term water yield impact of wildfire and other forest disturbance in eucalypt forests. *Environmental Modelling & Software*, *25*(4), 467–478. https://doi.org/10.1016/j.envsoft.2009.11.001

Lawler, R. R., & Link, T. E. (2011). Quantification of incoming all-wave radiation in discontinuous forest canopies with application to snowmelt prediction. *Hydrological Processes*, *25*(21), 3322–3331. https://doi.org/10.1002/hyp.8150

Lundberg, A., & Halldin, S. (2001). Snow interception evaporation. Review of measurement techniques, processes, and models. *Theoretical and Applied Climatology*, *70*(1-4), 117–133. WOS:000172271800010 https://doi.org/10.1007/s007040170010

Lundquist, J. D., & Cayan, D. R. (2007). Surface temperature patterns in complex terrain: Daily variations and long-term change in the central Sierra Nevada, California. *Journal of Geophysical Research*, *112*, D11124. https://doi.org/10.1029/2006JD007561

Lundquist, J. D., Dickerson-Lange, S. E., Lutz, J. A., & Cristea, N. C. (2013). Lower forest density enhances snow retention in regions with warmer winters: A global framework developed from plot-scale observations and modeling. *Water Resources Research*, *49*, 6356–6370. https://doi.org/10.1002/wrcr.20504

Lundquist, J. D., & Loheide, S. P. (2011). How evaporative water losses vary between wet and dry water years as a function of elevation in the Sierra Nevada, California, and critical factors for modeling. *Water Resources Research*, *47*, W00H09. https://doi.org/10.1029/2010WR010050

Lundquist, J. D., Pepin, N., & Rochford, C. (2008). Automated algorithm for mapping regions of cold-air pooling in complex terrain. *Journal of Geophysical Research*, *113*, D22107. https://doi.org/10.1029/2008JD009879

Maurer, E. P. (2007). Uncertainty in hydrologic impacts of climate change in the Sierra Nevada, California, under two emissions scenarios. *Climatic Change*, *82*(3), 309–325. https://doi.org/10.1007/s10584-006-9180-9

Mayor, A. G., Bautista, S., Llovet, J., & Bellot, J. (2007). Post-fire hydrological and erosional responses of a Mediterranean landscape: Seven years of catchment-scale dynamics. *CATENA*, *71*(1), 68–75. https://doi.org/10.1016/j.catena.2006.10.006

McLaughlin, B. C., Ackerly, D. D., Klos, P. Zion, Natali, J., Dawson, T. E., & Thompson, S. E. (2017). Hydrologic refugia, plants, and climate change. *Global Change Biology*, *23*, 2941–2961. https://doi.org/10.1111/gcb.13629

Micheletty, P., Kinoshita, A., & Hogue, T. (2014). Application of MODIS snow cover products: Wildfire impacts on snow and melt in the Sierra Nevada. *Hydrology & Earth System Sciences Discussions*, *11*(7), 7513–7549. https://doi.org/10.5194/hess-18-4601-2014

Miller, J. D., Collins, B. M., Lutz, J. A., Stephens, S. L., van Wagtendonk, J. W., & Yasuda, D. A. (2012). Differences in wildfires among ecoregions and land management agencies in the Sierra Nevada region, California, USA. *Ecosphere*, *3*(9), art80. https://doi.org/10.1890/ES12-00158.1

Miller, J. D., Safford, H. D., & Welch, K. R. (2016). Using one year post-fire fire severity assessments to estimate longer-term effects of fire in conifer forests of northern and eastern California, USA. *Forest Ecology and Management*, *382*, 168–183. https://doi.org/10.1016/j.foreco.2016.10.017

Miller, J. D., & Thode, A. E. (2007). Quantifying burn severity in a heterogeneous landscape with a relative version of the delta normalized burn ratio (dNBR). *Remote Sensing of Environment*, *109*(1), 66–80. https://doi.org/10.1016/j.rse.2006.12.006

Miller, C., & Urban, D. L. (2000). Modeling the effects of fire management alternatives on Sierra Nevada mixed-conifer forests. *Ecological Applications*, *10*(1), 85–94. https://doi.org/10.1890/1051-0761(2000)010[0085:MTEOFM]2.0.CO;2

Monteith, J. (1965). Evaporation and the environment, *Proceedings of the 19th Symposium of the Society for Experimental Biology* (pp. 205–233): Cambridge University Press.

Moody, J. A., & Martin, D. A. (2001). Post-fire, rainfall intensity–peak discharge relations for three mountainous watersheds in the western USA. *Hydrological Processes*, *15*(15), 2981–2993. https://doi.org/10.1002/hyp.386

Morgan, P., Hardy, C. C., Swetnam, T. W., Rollins, M. G., & Long, D. G. (2001). Mapping fire regimes across time and space: Understanding coarse and fine-scale fire patterns. *International Journal of Wildland Fire*, *10*(4), 329–342. https://doi.org/10.1071/WF01032

Neary, D., Ryan, K. C., & DeBano, L. F. (2005). Wildland fire in ecosystems: Effects of fire on soil and water. Rocky Mountain Research Station: United States Department of Agriculture. Forest Service. Retrieved from https://www.fs.fed.us/rm/pubs/rmrs\ignorespacesgtr042\ignorespaces4.pdf

Pierson, F. B., Robichaud, P. R., & Spaeth, K. E. (2001). Spatial and temporal effects of wildfire on the hydrology of a steep rangeland watershed. *Hydrological Processes*, *15*(15), 2905–2916. https://doi.org/10.1002/hyp.381

Prieto, I., Armas, C, & Pugnaire, F. I. (2012. Water release through plant roots: New insights into its consequences at the plant and ecosystem level. *New Phytologist*, *193*(4), 830–841. https://doi.org/10.1111/j.1469-8137.2011.04039.x

Roche, J. W., Goulden, M. L., & Bales, R. C. (2018). Estimating evapotranspiration change due to forest treatment and fire at the basin scale in the Sierra Nevada, California. *Ecohydrology*, *0*(0), e1978. https://doi.org/10.1002/eco.1978

Roy, J. W., & Hayashi, M. (2009). Multiple, distinct groundwater flow systems of a single moraine-talus feature in an alpine watershed. *Journal of Hydrology*, *373*(1–2), 139–150. https://doi.org/10.1016/j.jhydrol.2009.04.018

Saksa, P. (2015). Forest management, wildfire, and climate impacts on the hydrology of Sierra Nevada mixed-conifer watersheds (Ph.D. Thesis). UC Merced: Environmental Systems, 1030 https://escholarship.org/uc/item/90w5r5qs.

Saksa, P. C., Conklin, M. H., Battles, J. J., Tague, C. L., & Bales, R. C. (2017). Forest thinning impacts on the water balance of Sierra Nevada mixed-conifer headwater basins. *Water Resources Research*, *53*, 5364–5381. https://doi.org/10.1002/2016WR019240

Seibert, J., & McDonnell, J. J. (2002). On the dialog between experimentalist and modeler in catchment hydrology: Use of soft data for multicriteria model calibration. *Water Resources Research*, *38*(11), 1241. https://doi.org/10.1029/2001WR000978

Seibert, J., McDonnell, J. J., & Woodsmith, R. D. (2010). Effects of wildfire on catchment runoff response: A Modelling approach to detect changes in snow-dominated forested catchments. *Hydrology research*, *41*(5). https://doi.org/10.2166/nh.2010.036

Stephens, S. L., Fry, D. L., & Franco-Vizcaño, E. (2008). Wildfire and spatial patterns in forests in northwestern Mexico: The United States wishes it had similar fire problems. *Ecology and Society*, *13*(2).

Stevens, J. T. (2017). Scale-dependent effects of post-fire canopy cover on snowpack depth in montane coniferous forests. *Ecological Applications*, *27*, 1888—900. https://doi.org/10.1002/eap.1575

Svoma, B. M. (2017). Canopy effects on snow sublimation from a central Arizona basin. *Journal of Geophysical Research: Atmospheres*, *122*, 20–46. https://doi.org/1002/2016JD025184

Tague, C. L., & Band, L. E. (2004). RHESSys: Regional hydro-ecologic simulation system—An object-oriented approach to spatially distributed modeling of carbon, water, and nutrient cycling. *Earth Interactions*, *8*(1). https://doi.org/10.1175/1087-3562(2004)8h1:RRHSSOi2.0.CO;2

Tague, C., & Dugger, A. L. (2010). Ecohydrology and climate change in the mountains of the western USA—A review of research and opportunities. *Geography Compass*, *4*(11), 1648–1663. https://doi.org/10.1111/j.1749-8198.2010.00400.x

Tague, C., & Grant, G. E. (2009). Groundwater dynamics mediate low-flow response to global warming in snow-dominated alpine regions. *Water Resources Research*, *45*, W07421. https://doi.org/10.1029/2008WR007179

Tague, C. L., Moritz, M., & Hanan, E. (2019). The changing water cycle: The eco-hydrologic impacts of forest density reduction in Mediterranean (seasonally dry) regions. *Wiley Interdisciplinary Reviews: Water*, *0*, e1350. https://doi.org/10.1002/wat2.1350

Tague, C., & Peng, H. (2013). The sensitivity of forest water use to the timing of precipitation and snowmelt recharge in the California Sierra: Implications for a warming climate. *Journal of Geophysical Research: Biogeosciences*, *118*, 875–887. https://doi.org/10.1002/jgrg.20073

Tennant, C. J., Harpold, A. A., Lohse, K. A., Godsey, S. E., Crosby, B. T., Larsen, L. G., et al. (2017). Regional sensitivities of seasonal snowpack to elevation, aspect, and vegetation cover in western North America. *Water Resources Research*, *53*, 6908–6926. https://doi.org/10.1002/2016WR019374

Tesfa, T. K., Tarboton, D. G., Chandler, D. G., & McNamara, J. P. (2009). Modeling soil depth from topographic and land cover attributes. *Water Resources Research*, *45*, W10438. https://doi.org/10.1029/2008WR007474

Trujillo, E., & Molotch, N. P. (2014). Snowpack regimes of the western United States. *Water Resources Research*, *50*, 5611–5623. https://doi.org/10.1002/2013WR014753

Ursino, N., & Rulli, M. C. (2011). Hydrological minimal model for fire regime assessment in a Mediterranean ecosystem. *Water Resources Research*, *47*, W11526. https://doi.org/10.1029/2011WR010758

van Wagtendonk, J. W. (2007). The history and evolution of wildland fire use. *Fire Ecology*, *3*, 3–17. https://doi.org/10.4996/fireecology.0302003

Vieira, D. C. S., Fernandez, C., Vega, J. A., & Keizer, J. J. (2015). Does soil burn severity affect the post-fire runoff and interrill erosion response? A review based on meta-analysis of field rainfall simulation data. *Journal of Hydrology*, *523*, 452–464. https://doi.org/10.1016/j.jhydrol.2015.01.071

Westerling, A., & Bryant, B. (2008). Climate change and wildfire in California. *Climatic Change*, *87*(1), 231–249. https://doi.org/10.1007/s10584-007-9363-z

Wine, M. L., & Cadol, D. (2016). Hydrologic effects of large southwestern USA wildfires significantly increase regional water supply: Fact or fiction? *Environmental Research Letters*, *11*(8), 85006. https://doi.org/10.1088/1748-9326/11/8/085006